Journal of King Saud University – Science 33 (2021) 101579

Contents lists available at ScienceDirect

Journal of King Saud University – Science

journal homepage: www.sciencedirect.com

Original article

Decolourization of malachite green dye by endolichenic fungi from the lichen *Usnea* sp.: A novel study on their dye removal potential

Adeline Su Yien Ting *, Chloe Kai Wai Cheng, Krystle Angelique Aguda Santiago

School of Science, Monash University Malaysia, Jalan Lagoon Selatan, 47500 Bandar Sunway, Selangor Darul Ehsan, Malaysia

ARTICLE INFO

Article history:
Received 21 September 2020
Revised 11 August 2021
Accepted 17 August 2021
Available online 25 August 2021

Keywords:
Decolorization
Endolichenic fungi
FTIR
Malachite green

ABSTRACT

Objective: This novel study explored the potential of two endolichenic fungi, *Pseudopestalotiopsis theae* (PT, accession number MG881833) and *Astrocystis bambusae* (AB, accession number MH370741) in decolorizing Malachite Green (MG).
Methods: Their efficacy in dye decolorization was compared to non-endolichenic fungus *Trichoderma asperellum* (TA, accession number KP792512). Decolorization test was performed using MG (100 ppm) for 14 days (absorbance at 617 nm) to determine decolorization efficiency (DE, %). The pellet was collected for FTIR analysis (4000 to 700 cm^{-1}, 50-scan speed) while the supernatant was analysed with UV-spectral analysis (300–800 nm) to detect for biodegradation.
Results: P. theae demonstrated the highest decolorization efficiency (DE%) at 89.22%, followed by *T. asperellum* (76.19%) and *A. bambusae* (67.69%). Common functional groups (i.e., —OH, —COOH, —NH, —CH, C═O, ═C—H) were detected in all isolates and their roles in biosorption were evident by the shifts in peaks and peak intensity. Biodegradation of MG was concluded based on UV-spectra peaks at 617 nm, which were significantly reduced (or absent).
Conclusion: This study is the first to reveal that endolichenic fungi *P. theae* and *A. bambusae* are capable of decolorizing the toxic dye malachite green.

1. Introduction

Endolichenic fungi (ELF) are found in lichens and are ubiquitous in the environment. They have been recovered from lichen species across a vast geographical region; from the Arctic and Antarctic regions to the tropics (Arnold et al., 2009; Kannangara et al., 2009; U'ren et al., 2010; Suryanarayanan et al., 2017). Existing reports suggested ELF predominantly comprise of species of Ascomycota (Pezizomycotina) (U'ren et al., 2010; Kellogg and Raja, 2017), Basidiomycota and Zygomycota (Tripathi and Joshi, 2015). Examples of common ELF include *Aspergillus versicolor* (Li et al., 2015), *Penicillium* sp. and *Chrysosporium* sp. (Kannangara et al., 2009).

The ELF are similar to the endophytic fungi based on species identified, transmission mode, phylogenetic relationship and evolutionary history (Arnold et al., 2009; Hawas et al., 2012; Waqas et al., 2014). The two ELF in this study, *Pseudopestalotiopsis theae* (PT) and *Astrocystis bambusae* (AB), are known endophytes (Peláez et al., 2008; Maharachchikumbura et al., 2014; Dai et al., 2017) but their nature as ELF is novel. In addition, ELF has not been explored for bioremediation, although they are valued for their metabolites (e.g. xanthones, alkaloids, quinones, anthraquinones, pyrones, furanones, steroids and benzopyranoids) (Wang et al., 2012; Dou et al., 2014; Zheng et al., 2014; Santiago and Ting, 2019).

This study therefore, aims to establish the potential of ELF in removing toxic dyes, particularly triphenylmethane (TPM) dyes. TPM dyes are cationic, N-methylated diaminotriphenylmethane dyes, used extensively for various industries (printing, textile, food, paper), and include the malachite green dye (MG) (Chen et al. 2019). MG is toxic and carcinogenic and although biological

Abbreviations: AB, *Astrocystis bambusae*; ANOVA, One-way Analysis of Variance; DE, decolorization efficiency; ELF, Endolichenic fungi; FTIR, Fourier transformed infra-red; MG, malachite green; PDA, potato dextrose agar; PDB, potato dextrose broth; PT, *Pseudopestalotiopsis theae*; SPSS, Statistical Package for the Social Science; TA, *Trichoderma asperellum*; UV–vis, ultraviolet visible.

* Corresponding author.
E-mail addresses: adeline.ting@monash.edu, adelsuyien@yahoo.com (A.S.Y. Ting).

Peer review under responsibility of King Saud University.

Production and hosting by Elsevier

https://doi.org/10.1016/j.jksus.2021.101579

removal of MG has been attempted using non-endolichenic fungi (Chen and Ting, 2015a; 2015b), exploration using ELF remains novel. The potential use of ELF for bioremediation is associated with their lichen hosts. Kulkarni et al. (2014) used the lichen *Permelia perlata* to decolorize (80.4% decolorization efficiency, DE) Solvent Red 24. In another study, the lichen *Dermatocarpon vellereceum* decolorized Navy Blue HE22 (87.4% DE) (Kulkarni et al., 2018). Dye degradation by these lichens was attributed to the enzymes laccase, manganese peroxidase and lignin peroxidase. However, as lichens are extremely slow-growing, ELF are sought as alternatives to decolorize dyes, especially with reports that ELF are capable of secreting similar enzymes as their lichen hosts (Kannangara et al., 2009; Beckett et al., 2013).

This study embarks on discovering the dye degradation potential of two ELF species (*Pseudopestalotiopsis theae* and *Astrocystis bambusae*), and their potential for removal of MG dye. ELF are explored as their lichen host have shown good potential for dye remediation. Furthermore, ELF are similar to endophytes, and may have similar dye degrading potential as endophytes. Therefore, in this study, the efficacy of the ELF is compared against a non-endolichenic fungus, *Trichoderma asperellum,* which is an endophyte. This will be one of the first attempts in realizing the dye degradation activities of ELF.

2. Materials and methods

2.1. Culture establishment and generation of fungal biomass

The ELF *Pseudopestalotiopsis theae* (PT, accession number MG881833) and *Astrocystis bambusae* (AB, accession number MH370741) were obtained as pure stock cultures. These isolates were isolated from the lichen *Usnea pectinata* (Sagada Mountain Province, Philippines) and *U. bismolliuscula* (Bukit Larut, Perak, Malaysia), respectively. The non-endolichenic fungus *Trichoderma asperellum* (TA, accession number KP792512) was also obtained as stock culture, previously been isolated from *Phragmites* sp., a phytoremediator plant (Sim et al., 2016). The isolates were cultured on potato dextrose agar (PDA, Friendemann Schmidt) and incubated at room temperature (RT, 25 ± 2 °C). To generate biomass, ten mycelial plugs (5 mm diameter) of each isolate were inoculated into 250 mL potato dextrose broth (PDB, Friendemann Schmidt) and incubated (100 rpm, RT) (Innova 44 stackable incubator shaker, New Brunswick Scientific) for 5 days or until sufficient biomass is attained (Chew and Ting, 2016). The mycelium was then harvested via filtration through sterile cheesecloth, rinsed with sufficient amount of distilled water, and weighed to 0.5 g fresh weight (Macharchand and Ting, 2017). The fresh biomass was used for subsequent experiments.

2.2. Dye decolorization activities

Malachite Green (MG) (CAS-No.2437–29-8, Friendemann Schmidt) dye was added into 25 mL autoclaved MilliQ water (18.2 MΩ, Sartorius, Malaysia) to produce the dye solution (100 ppm concentration). The fresh fungal biomass (0.5 g) (from section 2.1) was then inoculated into the dye solution and incubated for 14 days (25 ± 2 °C, 120 rpm). Non-inoculated (untreated) MG solution was assigned as negative control and incubated similarly. For every 24 h-interval (until day 14), 2 mL of dye solution was pipetted and centrifuged (10,000 rpm, 10 min), and the absorbance of the supernatant read at 617 nm (Tecan Spark M10 plate reader). The pellet was collected for FTIR analysis. The procedure was repeated for all isolates and the decolorization efficiency (DE, %) (Equation 1) was determined as follows:

$$\text{Decolorization efficiency (DE, \%)} = [(A_i - A_o)/A_i] \times 100\%$$

where A_i represented initial absorbance and A_o for observed absorbance upon treatment with the isolates (Macharchand and Ting, 2017).

2.3. Ultraviolet–visible (UV–vis) spectral analysis for detection of biodegradation potential

Fresh fungal biomass (0.5 g) was introduced into 25 mL of MG solution, and incubated for 14 days (100 rpm, RT). Non-treated dye solution was assigned as negative control and incubated similarly. Two mL of aliquot was withdrawn every 24-h interval for the next 14 days. The suspension was centrifuged (10,000 rpm, 10 min) and the absorbance of the supernatant was measured (300 to 800 nm) with a UV–vis spectrophotometer (UviLine 9400, Secomam). The UV–vis spectra peaks (day 1–14) for treated and non-treated (control) MG solutions were then plotted and compared (Macharchand and Ting, 2017).

2.4. FTIR-analysis of fungal biomass in Malachite Green solution

The biomass of AB, PT and TA were collected at day 1 and 8 from treated solutions (Section 2.2). The pellet obtained was oven-dried (50 °C) overnight, and ground into powder form using pestle and mortar. Single-reflection attenuated total reflection spectra (within 4000–400 cm^{-1}) was obtained using the FTIR spectrometer conducted under ambient temperature. Data were collected within the mid-infrared region from 4000 to 700 cm^{-1} (50-scan speed) to exclude interference (Chew and Ting, 2016).

2.5. Statistical analysis

Each experiment was conducted in triplicates, and the data analysed with One-way Analysis of Variance (ANOVA) using Statistical Package for the Social Science (SPSS) version 22.0 (IBM). Means were compared using Tukey's Test (Honestly Significant Difference, $HSD_{(0.05)}$).

3. Results

3.1. Decolorization of Malachite Green dye

All three isolates decolorized MG, resulting in hues of bluish green. The isolate *P. theae* (PT) was most effective with significantly highest DE (71.42%), compared to *T. asperellum* (TA) (64.16% DE)

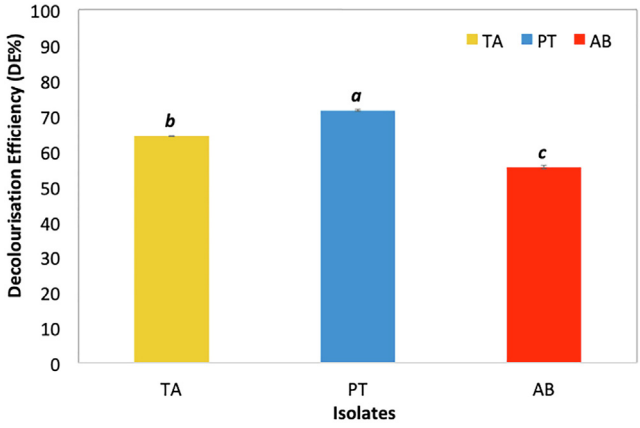

Fig. 1. Decolourisation efficiency (DE%) of *T. asperellum* (TA), *P. theae* (PT) and *A. bambusae* (AB) on Malachite Green (MG) (100 mg L^{-1}). Mean comparisons with the same letter and font type are not significantly different according to Tukey's Test ($HSD_{0.05}$). Error bars indicate standard deviation of means.

and *A. bambusae* (AB) (55.39% DE) (Fig. 1). A difference of 7.26% in DE was observed for PT and TA. Decolorization of MG by PT was also more effective compared to AB, resulting in a difference of 16.03% in DE.

The dye decolorization rate was, however, more rapidly observed when TA was used for dye treatment. The DE was increasing significantly for the first 4 days, with maximum DE attained by day 4 (66.77%). On the contrary, dye decolorization by both ELF (PT, AB) were less rapid than TA. Decolorization activities peaked at day 5 for both isolates (79.27% and 55.14%, for PT and AB, respectively) (Fig. 2). By day 14, PT demonstrated the highest DE with 89.22% DE, compared to TA (76.19% DE) and AB (67.69% DE) (Fig. 2).

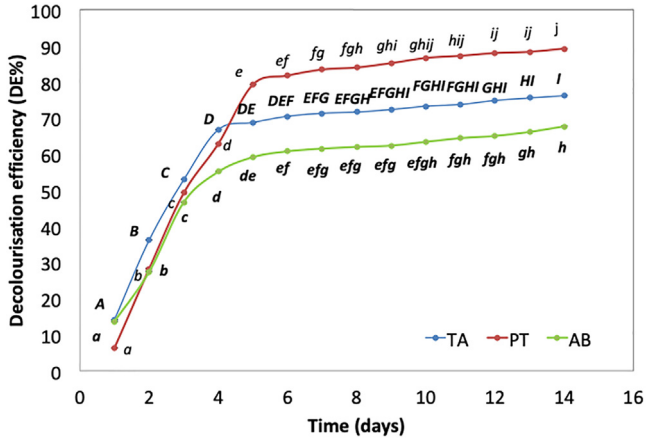

Fig. 2. Decolourisation efficiency (DE%) of *T. asperellum* (TA), *P. theae* (PT) and *A. bambusae* (AB) on Malachite Green (MG) (100 mg L^{-1}). Mean comparisons with the same letter and font type are not significantly different according to Tukey's Test ($HSD_{0.05}$). Comparisons are made across time (days) within the same isolate. Error bars indicate standard deviation of means.

3.2. UV–vis spectra

By day 1, the spectra peak for MG (at 617 nm) treated with TA (absorbance = 2.008) had the lowest absorbance compared to AB (absorbance = 2.099) and PT (absorbance = 2.381). Spectrum for negative control (untreated MG) remained the highest (absorbance = 2.568) (Fig. 3). By day 14, the untreated MG solution retained the absorbance peak at 617 nm (absorbance = 2.499), but treatment with PT (absorbance = 0.271), TA (absorbance = 0.581) and AB (absorbance = 0.753) showed diminished peaks (Fig. 3). The UV–vis spectra suggested possible degradation of MG as the dye chromophore was no longer detected. PT was concluded to have the most potential for biodegradation of MG dye (Fig. 3).

3.3. FTIR spectra

The FTIR spectra for TA, PT and AB revealed the presence of additional functional groups (1000–2000 cm^{-1}) detected post-treatment in MG (Figs. 4–6). The major functional groups detected were hydroxyl (—OH), carboxyl (—COOH), amine (—NH) and alkane

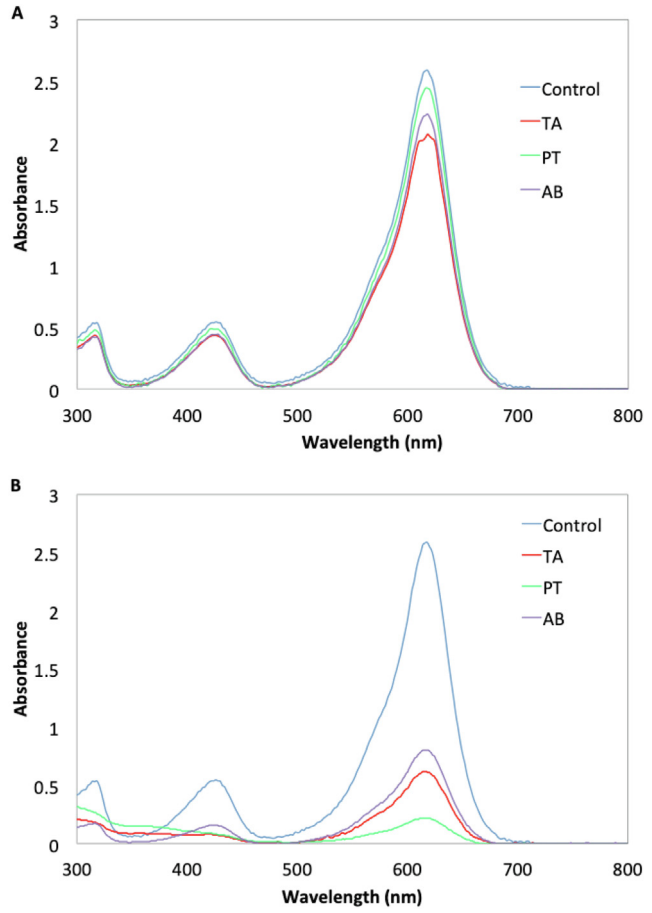

Fig. 3. UV–vis spectra of Malachite Green (MG) (100 mg L^{-1}) at (A) day 1 and (B) day 14 after treatment with *T. asperellum* (TA), *P. theae* (PT) and *A. bambusae* (AB). Spectra for control (non-inoculated/untreated) MG solution is included.

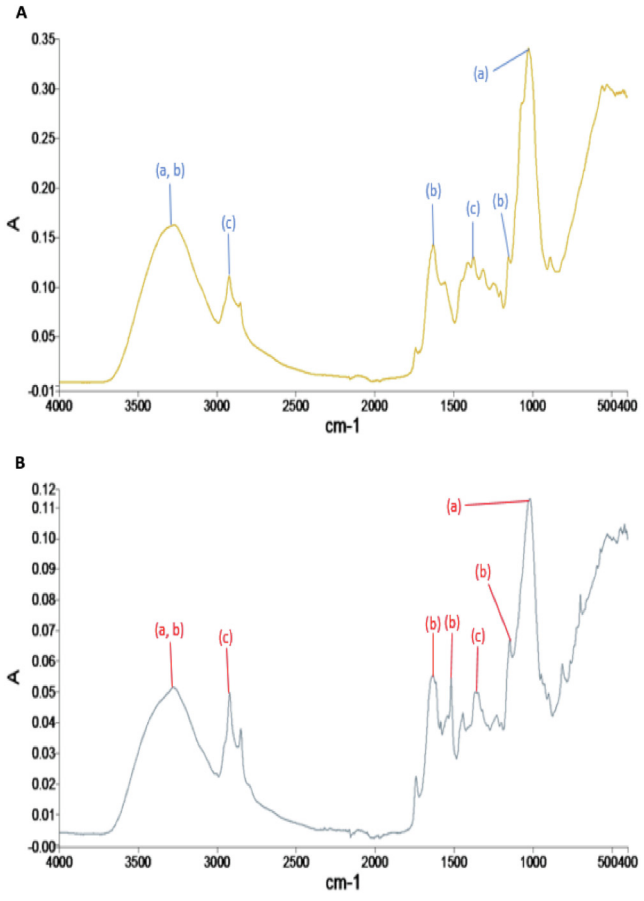

Fig. 4. FTIR spectra analysis of *A. bambusae* (AB) (A) at day 1 and (B) day 14 after inoculation for the treatment of Malachite Green (MG) solutions. For each of the peaks, the following primary functional groups are detected; (a) hydroxyl, (b) amine and (c) alkanes.

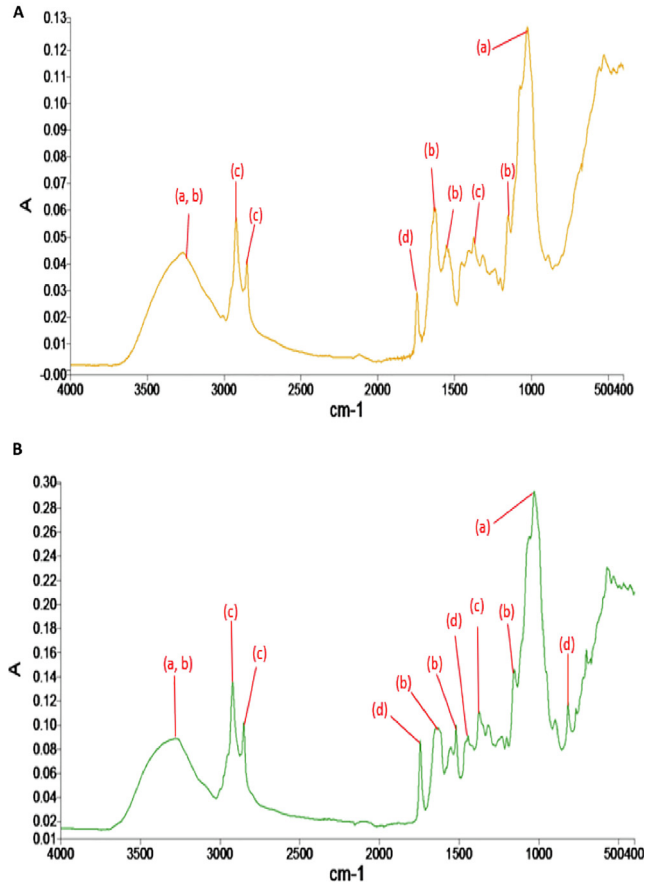

Fig. 5. FTIR spectra analysis of *T. asperellum* (TA) (A) at day 1 and (B) day 14 after inoculation for the treatment of Malachite Green (MG solutions). For each of the peaks, the following primary functional groups are detected; (a) hydroxyl, (b) amine, (c) alkanes and (d) other groups.

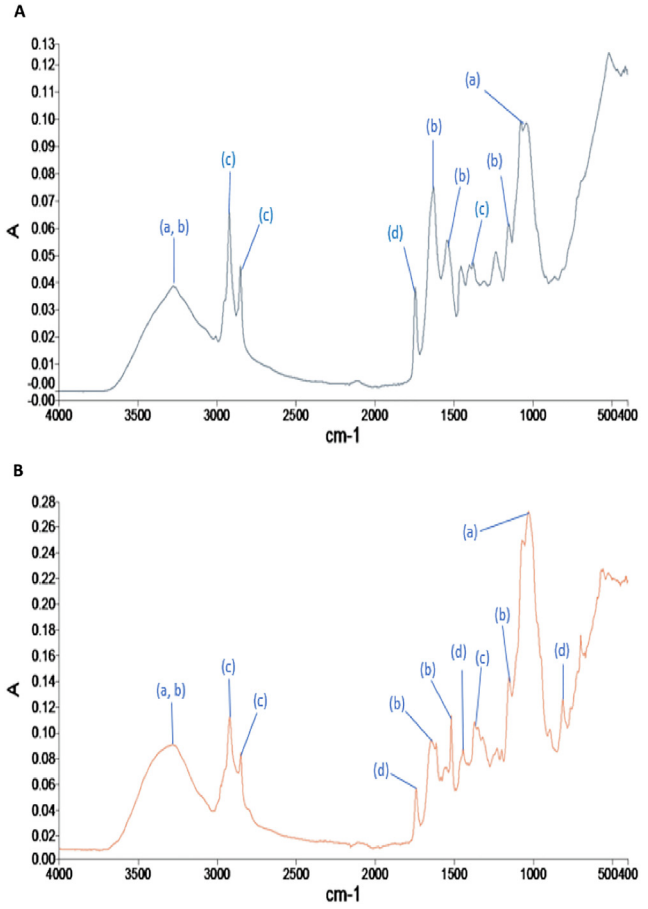

Fig. 6. FTIR spectra analysis of *P. theae* (PT) (A) at day 1 and (B) day 14 after inoculation for the treatment of Malachite Green (MG solutions). For each of the peaks, the following primary functional groups are detected; (a) hydroxyl, (b) amine, (c) alkanes and (d) other groups.

(—CH). Other functional groups observed include the stretching of C=O in esters (peaks at 1745.26 cm^{-1}) and =C—H bending in aromatic rings (peaks at 815.49 cm^{-1}) (Supplementary File-Table S1-S6). The FTIR spectra also revealed that AB in natural form (pre-treatment with MG), have lesser functional groups (~4 major groups) (Fig. 4) compared to TA (~6 major groups) (Fig. 5) and PT (~6 major groups) (Fig. 6). The number of major functional groups for AB remained the lowest of the three isolates, even post-treatment, with only ~ 5 major groups detected compared to ~ 8 major groups for both TA and PT (Figs. 4–6).

For AB, the bands representing the stretching of C=O in esters and =C—H bending in aromatic rings were absent (Fig. 4). Binding of MG to AB is ascribed to —OH and —NH (shifts from 3280.31 cm^{-1} to 3281.49 cm^{-1}), asymmetric CH_2— and CH_3— stretching vibrations (shifts from 2924.28 cm^{-1} to 2923.06 cm^{-1}) and CH_3 deformations (shifts from 1373.16 cm^{-1} to 1362.90 cm^{-1}) (Fig. 4). Bands at 1633.82 cm^{-1} (C=N and C=O stretching within the aromatic ring) shifted to 1634.77 cm^{-1}. A new peak observed at 1518.79 cm^{-1} (C—H bending in aromatic ring), suggested the possible binding of the MG dye to AB (Fig. 4).

The FTIR spectra for both PT and TA were similar. For PT, binding of MG was detected by shifts in peaks from 3278.01 cm^{-1} to 3275.21 cm^{-1} (hydroxyl (—OH) and amine (—NH)), from 2922.95 cm^{-1} to 2923.28 cm^{-1}, 2853.24 cm^{-1} to 2858.02 cm^{-1} (symmetric and asymmetric CH_2— and CH_3— stretching vibration), from 1374.26 cm^{-1} to 1372.96 cm^{-1} (CH_3 deformations) and emergence of peaks at 1518.20 cm^{-1} (C—H bending in aromatic ring) and 813.66 cm^{-1} (=C—H bending in aromatic ring) (Fig. 6). For TA, exposure to MG resulted in shifts for the hydroxyl (—OH) and amine (—NH) groups (from 3269.18 cm^{-1} to 3272.13 cm^{-1}) and for symmetric and asymmetric CH_2— and CH_3— stretching vibrations and CH_3 deformations from 2923.23 cm^{-1}, 2853.54 cm^{-1} and 1375.91 cm^{-1} to 2923.02 cm^{-1}, 2854.01 cm^{-1} and 1374.49 cm^{-1}, respectively (Fig. 5). New peaks were detected at 814.81 cm^{-1} (C—H bending in aromatic ring) after 14 days of treatment in MG.

To summarize, the FTIR spectra revealed that PT and AB shared similar major functional groups as the non-endolichenic TA. The number of functional groups may have a predisposition on the dye decolourization activities, as AB, which has the lowest number of functional groups, demonstrated lower dye decolourization efficiency and *vice versa*. Another critical observation is that new peaks were detected in all isolates post-treatment of MG, i.e. =C—H bending in aromatic ring (814.81 cm^{-1} or 813.66 cm^{-1}) for TA and PT, and C=C stretching vibration in the benzene ring (1518.20 cm^{-1} or 1518.19 cm^{-1}) for PT and AB. Isolate PT, with the highest decolourization activities, was discovered to have both these new peaks.

4. Discussion

This study has discovered that ELF have the potential to decolorize MG dye. *P. theae* (PT) is phylogenetically related to *Pestalotiopsis*, which has been reported to decolourize raw textile effluents of reactive dyes (~79.30 ± 1.70 % DE) (Verma et al.

2010). Interestingly, decolorization of MG by *A. bambusae* (AB) is reported for the first time. Although these ELF were isolated from pristine environments, they showed potential for dye removal, supporting their similarity to their lichen hosts and endophytes in removing dyes.

The dye decolorization efficiencies are presumably associated to the type and number of functional groups present. With lower number and types of functional groups found, poorer decolorization activities were observed. Hydroxyl (—OH), amine (—NH), alkane groups of symmetric and asymmetric CH2— and CH3— stretching vibration, CH3 deformations, C═N, C═O groups and C═C ring in lignin, or C═O in esters; are all responsible to bind cationic dyes (i.e. MG) via biosorption. Binding with dye molecules changes/shifts peaks of hydrogen bonds of functional groups (Zhang et al., 2011; Al Prol et al., 2017), while emergence of new peaks may arise from organic acids produced by fungi (Oberle-Kilic et al., 2013). The UV–vis spectra resonated with the FTIR results, suggesting ELF decolorized MG effectively. On the contrary, isolate *A. bambusae* (AB) which has lesser functional groups compared to *T. asperellum* (TA) and *P. theae* (PT) (absence of C═N and C═O stretching of carboxyl groups and C═C ring in lignin), demonstrated inferior decolorization activities.

From these observations, ELF is concluded to decolorize MG via biosorption and biodegradation as their main mechanisms. Biosorption occurs immediately as dye molecules bind to the functional groups present on the surface of fungal mycelium, reflected by the rapid decolorization rate, which plateaus once the binding sites are saturated and equilibrium is achieved (Khalaf, 2008; Rybczyńska-Tkaczyk and Korniłłowicz-Kowalska, 2016; Macharchand and Ting, 2017). Biodegradation involves enzymatic breakdown of the dyes evident by diminishing spectra peaks (Kaushik and Malik, 2009). Although enzymatic analyses were not performed, the differences in spectra peaks from the UV–vis analysis concurs that biodegradation through enzymatic processes likely occurred (Chen and Ting, 2015a, 2015b; Macharchand and Ting, 2017). Furthermore, *Pestalotiopsis* and *Trichoderma* have been profiled to produce enzymes related to biodegradation such as laccase, lignin-peroxidase or NADH-DCIP reductase (Verma et al., 2010; Shedbalkar and Jadhav, 2011; Macharchand and Ting, 2017). This study can benefit from further optimization studies to determine the optimum operational parameters for successful decolorization of MG. The toxicity of treated MG and the by-products produced can also be further examined. Although these are not investigated at this stage, previous studies using fungi have shown that optimum parameters are isolate dependent and treated dyes are often less toxic than original dye solutions observed from phytotoxicity tests (Chen and Ting, 2015a, 2015b; Chen et al., 2019).

5. Conclusion

This study revealed the dye decolorization potential of ELF (*P. theae* and *A. bambusae*). *P. theae* has better decolorization efficiency compared to the non-endolichenic *T. asperellum*, while *A. bambusae* was the least effective. The decolorization activities were attributed to both biosorption and biodegradation activities. Findings here highlighted the significant attributes of ELF, and their potential in decolorizing dyes. Further exploration into new bioremediative potential of ELF can be conducted in future.

Declaration of Competing Interest

The authors declare that they have no known competing financial interests or personal relationships that could have appeared to influence the work reported in this paper.

Acknowledgements

The authors extend their gratitude to Monash University Malaysia for the facilities to conduct the study.

Appendix A. Supplementary data

Supplementary data to this article can be found online at https://doi.org/10.1016/j.jksus.2021.101579.

References

Al Prol, A.E., El Moselhy, K.M., Kamel, M., Amer, A., Abdelmoneim, M., 2017. Bioremediation of Reactive Blue 19 and Reactive Black 5 from aqueous solution by using fungi *Aspergillus niger*. Int. J. Curr. Microbiol. Appl. Sci. 6 (3), 1676–1686. https://doi.org/10.20546/ijcmas.2017.603.193.

Arnold, A.E., Miadlikowska, J., Higgins, K.L., Sarvate, S.D., Gugger, P., Way, A., Hofstetter, V., Kauff, F., Lutzoni, F., 2009. A phylogenetic estimation of trophic transition networks for ascomycetous fungi: are lichens cradles of symbiotrophic fungal diversification? Syst. Biol. 58, 283–297. https://doi.org/10.1093/sysbio/syp001.

Beckett, R.P., Zavarzina, A.G., Liers, C., 2013. Oxidoreductases and cellulases in lichens: possible roles in lichen biology and soil organic matter turnover. Fungal Biol. 117 (6), 431–438. https://doi.org/10.1016/j.funbio.2013.04.007.

Chen, S.H., Cheow, Y.L., Ng, S.L., Ting, A.S.Y., 2019. Biodegradation of triphenylmethane dyes by non-white rot fungus *Penicillium simplicissimum*: enzymatic and toxicity studies. Int. J. Environ. Res. 13, 273–282. https://doi.org/10.1007/s41742-019-00171-2.

Chen, S.H., Ting, A.S.Y., 2015a. Biodecolorization and biodegradation potential of recalcitrant triphenylmethane dyes by *Coriolopsis* sp. isolated from compost. J. Environ. Manag. 150, 274–280. https://doi.org/10.1016/j.jenvman.2014.09.014.

Chen, S.H., Ting, A.S.Y., 2015b. Biosorption and biodegradation potential of triphenylmethane dyes by newly discovered *Penicillium simplicissimum* isolated from indoor wastewater sample. Int. Biodeter. Biodegrad. 103, 1–7. https://doi.org/10.1016/j.ibiod.2015.04.004.

Chew, S.Y., Ting, A.S.Y., 2016. Common filamentous *Trichoderma asperellum* for effective removal of triphenylmethane dyes. Desalin. Water Treat. 57 (29), 13534–13539. https://doi.org/10.1080/19443994.2015.1060173.

Dai, D.Q., Phookamsak, R., Wijayawardene, N.N., Li, W.J., Bhat, D.J., Xu, J.C., Taylor, J. E., Hyde, K.D., Chukeatirote, E., 2017. Bambusicolous fungi. Fungal Diver. 82, 1–105. https://doi.org/10.1007/s13225-016-0367-8.

Dou, Y.L., Wang, X., Jiang, D., Wang, H., Jiao, Y., Lou, H., Wang, X., 2014. Metabolites from *Aspergillus versicolor*, an endolichenic fungus from the lichen *Lobaria retigera*. Drug Discov. Ther. 8 (2), 84–88. https://doi.org/10.5582/ddt.8.84.

Hawas, U.W., El-Beih, A.A., El-Halawany, A.M., 2012. Bioactive anthraquinones from endophytic versicolor isolated from red sea algae. Archiv. Pharma. Res. 35, 1749–1756. https://doi.org/10.1007/s12272-012-1006-x.

Kannangara, B.T.S.D.P., Rajapaksha, R.S.C.G., Paranagama, P.A., 2009. Nature and bioactivities of endolichenic fungi in *Pseudocyphellaria* sp., *Parmotrema* sp. and *Usnea* sp. at Hakgala montane forest in Sri Lanka. Lett. Appl. Microbiol. 48, 203–209. https://doi.org/10.1111/j.1472-765X.2008.02512.x.

Kaushik, P., Malik, A., 2009. Fungal dye decolourization: recent advances and future potential. Environ. Int. 35 (1), 127–141. https://doi.org/10.1016/j.envint.2008.05.010.

Kellogg, J.J., Raja, H.A., 2017. Endolichenic fungi: a new source of rich bioactive secondary metabolites on the horizon. Phytochem. Rev. 16, 271–293. https://doi.org/10.1007/s11101-016-9473-1.

Khalaf, M.A., 2008. Biosorption of reactive dye from textile wastewater by non-viable biomass of *Aspergillus niger* and *Spirogyra* sp. Biores. Technol. 99 (14), 6631–6634. https://doi.org/10.1016/j.biortech.2007.12.010.

Kulkarni, A.N., Kadam, A.A., Kachole, M.S., Govindwar, S.P., 2014. Lichen *Permelia perlata*: a novel system for biodegradation and detoxification of disperse dye Solvent Red 24. J. Haz. Mater. 276, 461–468. https://doi.org/10.1016/j.jhazmat.2014.05.055.

Kulkarni, A.N., Watharkar, A.D., Rane, N.R., Jeon, B.H., Govindwar, S.P., 2018. Decolorization and detoxification of dye mixture and textile effluent by lichen *Dermatocarpon vellereceum* in fixed bed upflow bioreactor with subsequent oxidative stress study. Ecotoxicol. Environ. Saf. 148, 17–25. https://doi.org/10.1016/j.ecoenv.2017.10.001.

Li, X.-B., Zhou, Y.-H., Zhu, R.-X., Chang, W.-Q., Yuan, H.-Q., Gao, W., Zhang, L.-L., Zhao, Z.-T., Lou, H.-X., 2015. Identification and biological evaluation of secondary metabolites from the endolichenic fungus *Aspergillus versicolor*. Chem. Biodiv. 12, 575–592. https://doi.org/10.1002/cbdv.201400146.

Macharchand, S., Ting, A.S.Y., 2017. *Trichoderma asperellum* cultured in reduced concentrations of synthetic medium retained dye decolourization efficacy. J. Environ. Manag. 203, 542–549. https://doi.org/10.1016/j.jenvman.2017.06.068.

Maharachchikumbura, S.S.N., Hyde, K.D., Groenewald, J.Z., Xu, J., Crous, P.W., 2014. *Pestalotiopsis* revisited. Stud. Mycol. 79, 121–186. https://doi.org/10.1016/j.simyco.2014.09.005.

Oberle-Kilic, J., Dighton, J., Arbuckle-Keil, G., 2013. Atomic force microscopy and micro-ATR-FT-IR imaging reveals fungal enzyme activity at the hyphal scale of resolution. Mycol. 4 (1), 44–53. https://doi.org/10.1080/21501203.2012.759631.

Peláez, F., Gonzáles, V., Platas, G., Sánchez-Ballestero, J., Rubio, V., 2008. Molecular phylogenetic studies within the family Xylariaceae based on ribosomal DNA sequences. Fungal Diver. 31, 111–134.

Rybczyńska-Tkaczyk, K., Korniłłowicz-Kowalska, T., 2016. Biosorption optimization and equilibrium isotherm of industrial dye compounds in novel strains of microscopic fungi. Int. J. Environ. Sci. Technol. 13 (12), 2837–2846. https://doi.org/10.1007/s13762-016-1111-3.

Santiago, K.A.A., Ting, A.S.Y., 2019. Endolichenic fungi from common lichens as new sources for valuable bio-active compounds. In: Akhtar, M., Swamy, M., Sinniah, U. (Eds.), Natural Bio-active Compounds. Springer, Singapore, pp. 105–127.

Shedbalkar, U., Jadhav, J.P., 2011. Detoxification of malachite green and textile industrial effluent by *Penicillium ochrochloron*. Biotechnol. Bioproc. Eng. 16 (1), 196–204. https://doi.org/10.1007/s12257-010-0069-0.

Sim, C.S.F., Tan, W.S., Ting, A.S.Y., 2016. Endophytes from Phragmites for metal removal: evaluating their metal tolerance, adaptive tolerance behaviour and biosorption efficacy. Desalin. Water Treat. 57, 6959–6966. https://doi.org/10.1080/19443994.2015.1013507.

Suryanarayanan, T.S., Govindarajulu, M.B., Rajamani, T., Tripathi, M., Joshi, Y., 2017. Endolichenic fungi in lichens of Champawat District, Uttarakhand, Northern India. Mycol. Progress 16 (3), 205–211. https://doi.org/10.1007/s11557-016-1268-7.

Tripathi, M., Joshi, Y., 2015. Endolichenic fungi in Kumaun Himalaya: a case study. In: Upreti, D., Divakar, P., Shukla, V., Bajpai, R. (Eds.), Recent Adv. Lichenology. Springer, New Delhi, pp. 111–120.

U'Ren, J.M., Lutzoni, F., Miadlikowska, J., Arnold, A.E., 2010. Community analysis reveals close affinities between endophytic and endolichenic fungi in mosses and lichens. Microbial Ecol. 60 (2), 340–353. https://doi.org/10.1007/s00248-010-9698-2.

Verma, A.K., Raghukumar, C., Verma, P., Shouche, Y.S., Naik, C.G., 2010. Four marine-derived fungi for bioremediation of raw textile mill effluents. Biodegrad. 21 (2), 217–233. https://doi.org/10.1007/s10532-009-9295-6.

Wang, Q.X., Bao, L., Yang, X.L., Guo, H., Yang, R.N., Ren, B., Zhang, L.X., Dai, H.Q., Guo, L.D., Liu, H.W., 2012. Polyketides with antimicrobial activity from the solid culture of an endolichenic fungus *Ulocladium* sp. Fitoterapia 83 (1), 209–214. https://doi.org/10.1016/j.fitote.2011.10.013.

Waqas, M., Khan, A.L., Lee, I.J., 2014. Bioactive chemical constituents produced by endophytes and effects on rice plant growth. J. Plant Interact. 9 (1), 478–487. https://doi.org/10.1080/17429145.2013.860562.

Zhang, H., Tang, Y.i., Liu, X., Ke, Z., Su, X.i., Cai, D., Wang, X., Liu, Y., Huang, Q., Yu, Z., 2011. Improved adsorptive capacity of pine wood decayed by fungi *Poria cocos* for removal of malachite green from aqueous solutions. Desalin. 274 (1-3), 97–104. https://doi.org/10.1016/j.desal.2011.01.077.

Zheng, Q.C., Kong, M.Z., Zhao, Q., Chen, G.D., Tian, H.Y., Li, X.X., Guo, L.D., Li, J., Zheng, Y.Z., Gao, H., 2014. Chaetoglobosin Y, a new cytochalasan from *Chaetomium globosum*. Fitoterapia 93, 126–131. https://doi.org/10.1016/j.fitote.2013.12.022.